Geotechnical Aspects of Underground Construction in Soft Ground – Ng, Huang & Liu (eds)
© 2009 Taylor & Francis Group, London, ISBN 978-0-415-48475-6

Stability analysis of large slurry shield-driven tunnel in soft clay

Y. Li & Z.X. Zhang
Key Laboratory of Geotechnical and Underground Engineering of Ministry of Education, Tongji University, Shanghai, P.R. China
Department of Geotechnical Engineering, School of Civil Engineering, Tongji University, Shanghai, P.R. China

F. Emeriault & R. Kastner
INSA-Lyon, LGCIE, France

ABSTRACT: The possibility of partial failure of large slurry shield-driven tunnels is investigated by an upper-bound approach in limit analysis and a three-dimensional numerical modeling for the Shanghai Yangtze River Tunnel. The results of the upper-bound limit analysis failure mechanisms and the 3D numerical modeling have shown that the partial blow-out of the upper part of the tunnel face occurs when the slurry pressure is too large while the global collapse of the whole tunnel face occurs when the slurry pressure is too small. The failure mechanisms and critical slurry pressures obtained from both approaches are presented and discussed.

1 INTRODUCTION

In recent years, the rapid growth in urban development has resulted in an increased demand for the construction of tunnels for electric and communication cables, and transportation systems. For obvious practical reasons such as accessibility, serviceability and economy, these tunnels are constructed by shield machines of large diameter and at shallow depths. The Groene Hart Tunnel, constructed in 2005 in Netherlands, was carried out by a slurry-shield machine with an outside diameter of 14.87 m. The M-30 Tunnel in Madrid excavated by EPB shield machine, 15.2 m in diameter, was until recently the biggest shield tunnel completed in the world. In September 2006, two massive 15.43 m diameter slurry shield machines began work on Shanghai Yangtze River Tunnel. With the increase of the shield tunnel diameter, the excavated volume is increased dramatically and the probability of excavation in complicated stratum with different types of soil layers increases greatly too. The stability of the soil itself decreases at the same time. Thus, in recent years, more and more attention was paid to the face stability of large shield-driven tunnels.

The analysis of the face stability of shallow circular tunnels driven by the pressurized slurry shield requires the determination of the pressure to be applied by the shield. This pressure must avoid both the collapse (active failure) and the blow-out (passive failure) of the soil mass near the tunnel face. A number of studies have concerned tunnel face stability. Most results are analytical and are based on limit equilibrium method (Horn, 1961; Anagnostou & Kovári 1994; Broere, 2001) and limit analysis method (Davis et al. 1980; Leca & Dormieux, 1990; Chambon & Corté, 1994; Soubra 2000, 2002; Subrin & Wong, 2002). A rational and well-defined approach for the computation of the supporting pressure is translational multiblock failure mechanism of the upper-bound method, which is presented by Soubra (2002) based on the 3D limit analysis model of Leca and Dormieux (1990). This mechanism allows the slip surface to develop more freely in comparison with the available mechanisms given by Leca and Dormieux, and thus, improves the best upper-bound solutions given by these authors. The multiblock mechanism is convenient for a constant tunnel pressure which is an acceptable assumption for small to medium tunnel diameters ($\leq$10 m). However, studies on face stability of very large slurry shield-driven tunnels, for which the hypothesis of a constant slurry pressure is not applicable, are fairly few.

The non-constant supporting pressure of slurry shield-driven tunnel is caused by the density of the slurry. Since the density of the slurry should remain within a certain range to obtain high-quality filter cakes, and it is always smaller than the density of soil, there will be a pressure difference between the slurry pressure and the earth pressure at tunnel crown and invert. This pressure difference increases with the tunnel diameter increase, shown in Figure 1, where, S_u and S_b are the slurry pressures at the level of the tunnel crown and invert; P_u and P_b are the corresponding

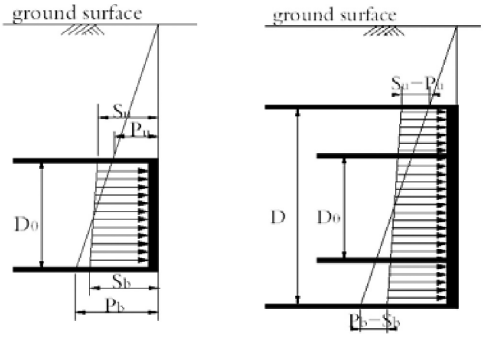

Figure 1. Pressure difference in different size tunnels.

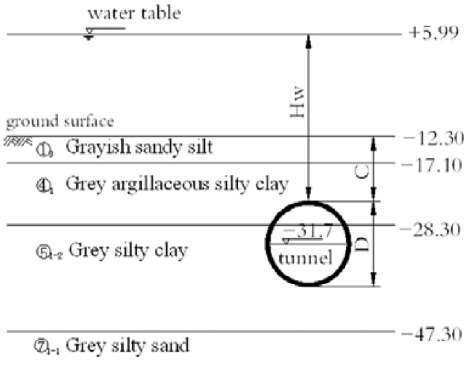

Figure 2. Geological condition with C/D = 0.7.

earth pressures; D_0 is the diameter of the small tunnel and D is the diameter of the larger one. This pressure difference may induce a different failure mechanism from the one corresponding to a constant slurry pressure, especially in large tunnels.

In this paper, a simplified computation scheme considering the non-constant slurry pressure is adopted, in which the multiblock failure mechanism suggested by Soubra (2002) is employed to investigate the possibility of partial failure in large size slurry shield-driven tunnel. Also, a more rigorous 3D numerical modeling is carried out to compare with the obtained results of critical slurry pressures and the corresponding soil mass at failure.

2 CASE STUDY

The main part of Shanghai Yangtze River Tunnel is 7.5 km river-crossing tunnel connecting the Pudong and Changxing Island in Shanghai, China. Excavation of the tunnels is carried out by a pressurized slurry shield machine with an outside diameter of 15.43 m, which is the world's largest until now.

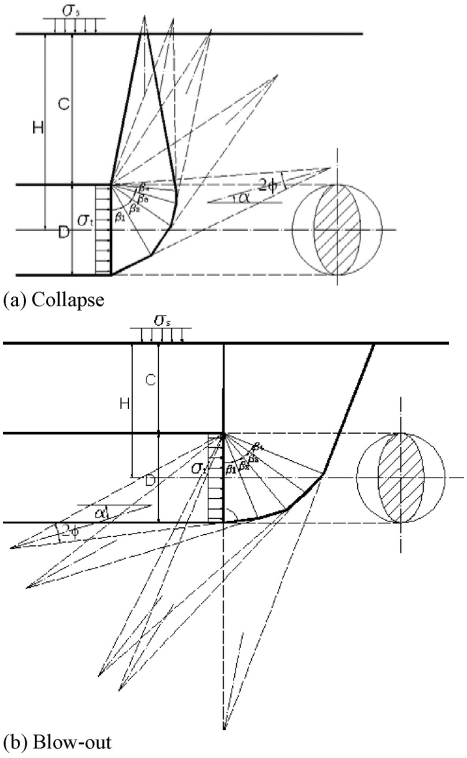

Figure 3. Multiblock failure mechanisms.

The tunnel is mainly excavated below the river bed of Yangtze River, which is composed of muddy clay and soft clay, with some local lenses of silty fine sand. The tunnel will be driven at a depth up to 65 m. A hydrostatic pressure up to 650 kPa is anticipated. The shallowest ground section is under the river with a cover-to-depth ratio of C/D = 0.7, where C and D is the cover depth and diameter of the tunnel. Because of the unfavorable geological condition and the large dimension of excavating face, the face stability of the tunnel is one of the key technical aspects in this project. The most dangerous profile with C/D = 0.7 is chosen for the study, as shown in Figure 2, where H_w is the height of the water table.

3 PARTIAL FAILURE MECHANISM

3.1 *Multiblock failure mechanism*

The problem of the face stability analysis relevant to a circular rigid tunnel of diameter *D* driven under a depth of cover *C* could be idealized, as shown in Figure 3. A surcharge σ_s is applied on the ground surface, and σ_t is the uniform supporting pressure on the tunnel face. The multiblock failure mechanism considered in this

paper is described in Soubra (2002). It is composed of several truncated rigid cones with circular cross-sections and with opening angles equal to 2ϕ, where ϕ is the friction angle of the soil. The different blocks of this mechanism move as rigid bodies. These rigid cones translate with velocities of different directions, which are collinear with the cones' axes and make an angle ϕ with the discontinuity surface. The velocity of each cone is determined by the condition that the relative velocity between the cones in contact has the direction that makes an angle ϕ with the contact surface. The present mechanism is completely defined by n angular parameters α and β_i (i = 1. . .n-1), where n is the number of rigid blocks. The geometrical construction of this mechanism is similar to that of Leca and Dormieux (1990). The present mechanism is characterized by more freedom angles than that of Leca and Dormieux (1990) and thus improves the solutions of the critical supporting pressure.

The external forces contributing to the rate of external work consist of (i) the self-weight of the truncated rigid cones; (ii) the surcharge loading σ_s (in case of outcrop of the upper rigid block) and (iii) the pressure σ_t at the face of the tunnel. The rate of energy dissipation occurs along the lateral surfaces and radial planes of the failure mechanism. By equating the total rate of external work to the total rate of internal energy dissipation, the pressure σ_t at the face of the tunnel is obtained as follow:

$$\sigma_t = N_s\sigma_s + (N_s - 1)\frac{c}{\tan\phi} + N_\gamma \gamma D \qquad (1)$$

where, N_s and N_γ are surcharge and soil weight coefficient; c, ϕ are the cohesion and friction angle of the soil and γ is the soil unit weight.

3.2 *Critical slurry pressures*

In order to study the possibility of partial failure, two partial failure mechanisms are used as shown in Figure 4, corresponding to the blow-out of the upper part of tunnel and the collapse of the lower part of tunnel. The partial failure is assumed to occur in an area with a vertical axis D_L, where $D_L \in (0, D)$. In upper part blow-out mechanism, as shown in Figure 4(a), the top of the failure area passes through the tunnel crown. In the lower part collapse mechanism, as shown in Figure 4(b), the bottom of the failure area passes through the tunnel invert. The upper part collapse and lower part blow-out are not considered because they are less dangerous.

The critical slurry pressure corresponding to partial upper part blow-out and lower part collapse are computed in a simplified approach using the multi-block failure mechanism as follow: the tunnel pressure obtained from the multiblock mechanism for different

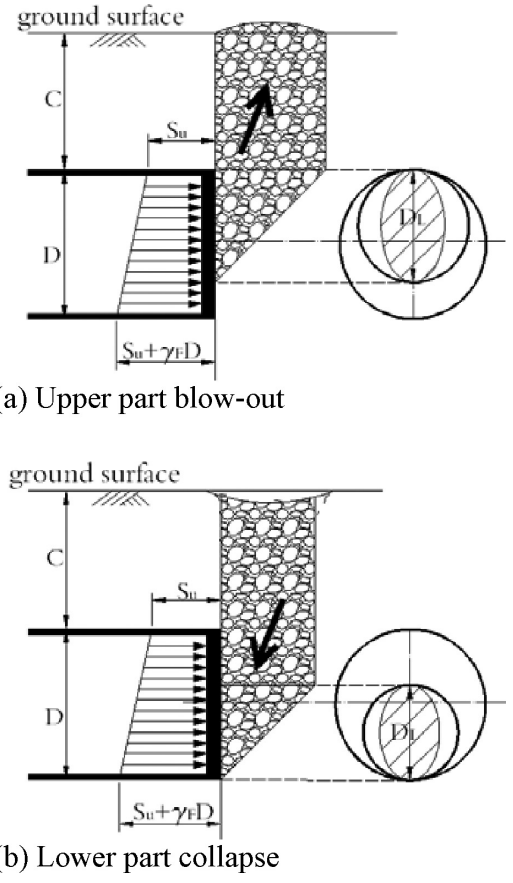

Figure 4. Two kinds of partial failure mechanisms.

prescribed values of the tunnel diameters (corresponding to different values of D_L in the present analysis) are computed. The value of D_L giving the minimal (respectively maximal) blow-out (respectively collapse) pressure is considered as the critical pressure causing a partial failure. A five-block model (i.e. $n = 5$) is employed for this study (as shown in Figure 3) since it was shown in Soubra (2002) that n greater than 5 will not significantly improve the results. Water above the ground surface is considered as a surcharge. Because the excavation is executed quickly compared to the soil consolidation, a typical undrained analysis is employed. Table 1 summarizes the characteristics of the soil. The unit weight of slurry is $\gamma_F = 12\,\mathrm{kN/m^3}$. In case 1, the cohesion is considered to be a constant. In case 2, cohesion of the soil increases with depth as $c_u = -0.95z + 0.4$, where z is the depth of the soil layer. The mean value from the level of tunnel invert to the ground surface in case 2 is equal to the c_u in case 1. Case 2 is chosen to take into account the variation of the undrained cohesion between the tunnel

Table 1. Soil parameters used in numerical modeling.

	unit weight γ_0 (kN/m^3)	cohesion c_u (kPa)	friction angle ϕ_u (°)	Young's modulus E (MPa)	Poisson's ratio ν
case1	18.2	24.5	0.01	3.21	0.495
case2	18.2	−0.95z+0.4	0.01	3.21	0.495

crown and invert in extra large tunnel, especially in normally consolidated clay.

According to the basic assumption of the multiblock failure mechanism, the intersection of the failure block and the tunnel face will be an ellipse with a long axis of D_L in vertical direction. The critical slurry pressure σ_{t0} obtained by multiblock model is a uniform pressure (as shown in Figure 3). Considering the total force balance on the failure face of diameter D_L, an equivalent slurry pressure is obtained. The slurry pressure σ_t at tunnel crown can be computed as follow: $\sigma_t = \sigma_{t0} - \gamma_s D_L/2$. Actually, since the slurry pressure increase with depth, the total force due to the slurry is acting on the tunnel face with eccentricity e. When using uniform pressure σ_{t0}, a moment should be taken into consideration at the same time. However, the moment is not considered here since the normalized eccentricity e/D is very small in this study (about 2%∼4%).

The critical slurry pressure σ_t is calculated for partial diameter D_L varying in 1 m steps, which leads to the maximum (or minimum) value of σ_t, as shown in Figure 5. In case 2, the cohesion for different D_L is the mean value from the top to the bottom of the failure block. In upper part blow-out, cohesion decreases with the decrease of D_L, since the failure block becomes more and more shallow. While in lower part collapse, the failure block is always starting from the tunnel invert to the ground surface, the mean value of cohesion for different D_L is equal to the one in case 1. Therefore, there is no difference between the value of σ_t in case 1 and 2 in collapse.

Figure 5 shows that in case 1, the maximum and minimum critical slurry pressure is obtained when partial failure diameter $D_L = D = 15.43$ m, which means that the global failure will happen both in collapse and blow-out cases.

In case 2, the minimum slurry pressure in blow-out is obtained when partial failure diameter is 12 m, which means that in blow-out failure, the partial failure of upper part tunnel face will be more dangerous than the global failure of the whole tunnel face. However, there are no great differences among critical slurry pressures when $D_L \in (10, 15.43)$. Therefore, in practice, global failure of the entire face and partial failure with $D_L > 10$ m will have the same probability. For collapse, the maximum slurry pressure is obtained when

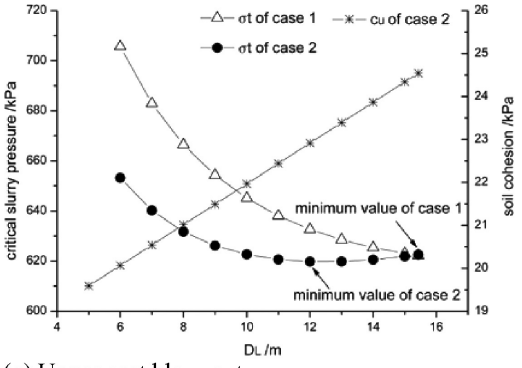

(a) Upper part blow-out

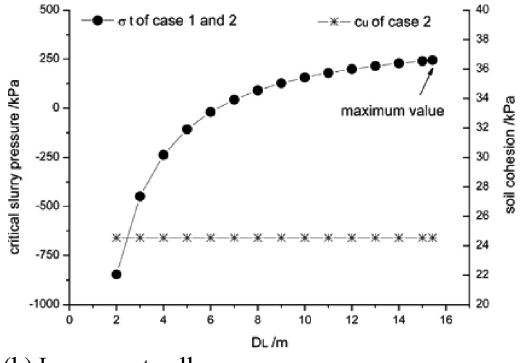

(b) Lower part collapse

Figure 5. Critical slurry pressure of partial failure mechanism.

$D_L = 15.43$ m. With the decrease of the partial failure diameter, the critical slurry pressure will decrease at the same time: global failure of the whole tunnel face is more dangerous than partial failure. The critical slurry pressure at the tunnel crown level is 619.9 kPa and 265.9 kPa corresponding to blow-out (partially) and collapse (globally), which is 712.5 kPa and 358.5 kPa at the level of tunnel center.

4 NUMERICAL ANALYSIS WITH FLAC^{3D}

4.1 *FLAC^{3D} numerical modeling*

In order to investigate the behavior of the tunnel face during failure, numerical analysis is carried out with the commercially available finite-difference code FLAC^{3D}, which is an effective program for situations where physical instability may occur.

In the model, due to symmetry, only one half is included. The model is sufficiently large to allow for any possible failure mechanism to develop and to avoid any influence from the model boundaries (as shown in Figure 6). The water table is 2D above the tunnel crown. In order to focus the analysis on

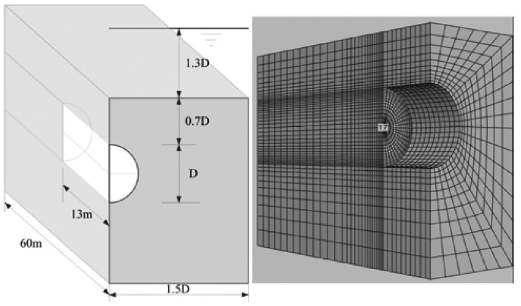

Figure 6. Studying profile and 3D numerical model.

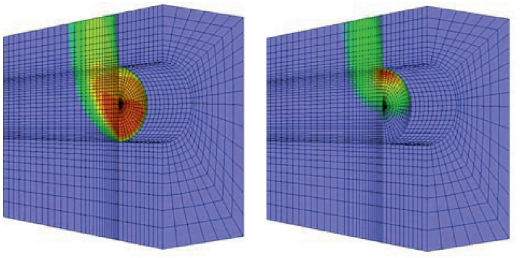

(a) Collapse (M=0.70) (b) Blow-out (M=1.30)

Figure 7. Displacement contours when failure is observed in case 2.

the face failure in front of the shield machine, the excavation process was simulated using a simplified single-step excavation scheme, assuming that the tunnel is excavated 13 m (the length of the shield machine) instantaneously. Such a simplified modeling scheme had been successfully adopted in previous studies (Gioda & Swoboda, 1999).

The different soil layers are assumed to be elastic perfectly-plastic materials conforming to the Mohr-Coulomb failure criterion. An undrained analysis is carried out by using the undrained parameters of the soil as shown in Table 1.

The initial slurry pressure σ_{s0} is equal to the earth pressure at rest at center of tunnel face (in this case, $\sigma_{s0} = 537.6$ kPa). The slurry pressure is increasing with the depth according to the density of the slurry. Slurry pressure at the center of the tunnel face σ_{si} will be increased (or decreased) by multiplying σ_{s0} by a pressure factor M in every construction phase i, until blow-out (or collapse) occurs. The failure criterion is defined as follows: the construction phase is considered as the beginning of failure, where for the first time considerable value of unbalance force (not equal to 0) and velocity (greater than $e^{-11} \sim e^{-12}$ m/step in this case) is observed. Then the critical slurry pressure corresponding to collapse and blow-out will be obtained by the following equation:

$$\sigma_{si} = M \cdot \sigma_{s0} \tag{2}$$

4.2 *Numerical modeling results*

For case 1, collapse occurs at the construction phase when $M = 0.65$ and blow-out occurs at $M = 1.30$; $M = 0.70$ and $M = 1.30$ for case 2 respectively. Maximum and minimum critical slurry pressure could be obtained by equation (2). Displacement contours at the failure of case 2 is plotted in Figure 7. A global collapse failure of the whole tunnel face is observed. This mechanism is well coincident with the centrifugal experiment result of Chambon and Corté (1994). However failure mechanism of blow-out is a partial failure

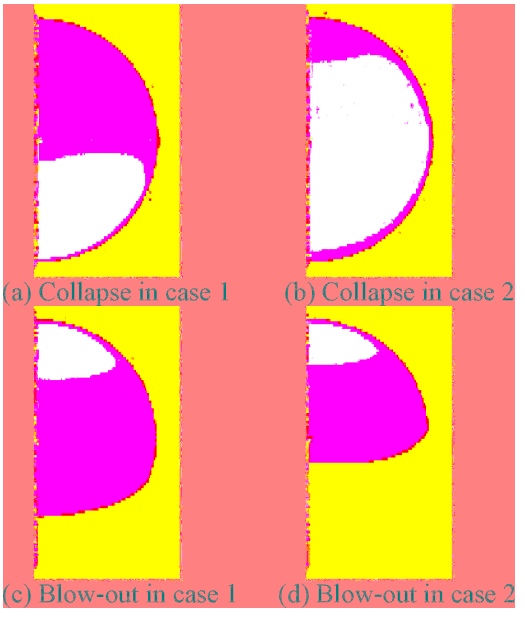

Figure 8. Velocity contours of tunnel face when failure occurs.

in the upper part of the tunnel face. Partial failure mechanism is more obvious in case 2 than in case 1.

Two cases are compared in Figure 8. In collapse, as shown in Figure 8 (a) and (b), the total tunnel face will have considerable value of velocity; and the most dangerous point with maximum velocity is near the tunnel invert. The failure area on the tunnel face is the whole face, which is circular in shape. In blow-out, as we see in Figure 8 (c) and (d), the failure is constrained in upper 3/4D and 1/2D part of the tunnel face, corresponding to the case 1 and case 2 respectively. The failure mechanism in both cases has an elliptic shape, with a long axis in the horizontal direction. The most dangerous point with the maximum velocity is the point near the tunnel crown. The failure mechanism of case 2 could be obviously observed by the plot of

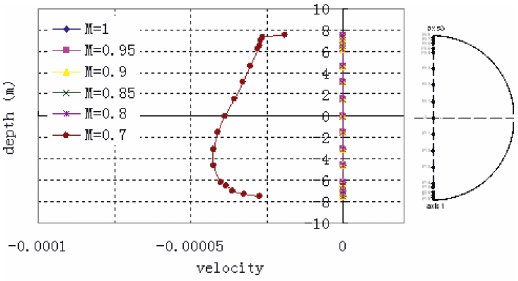

(a) Collapse

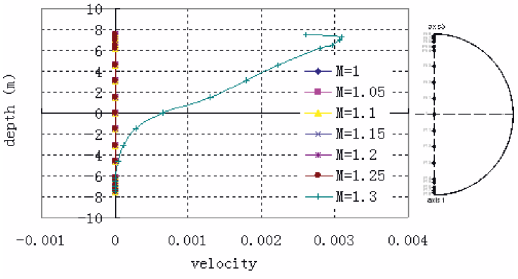

(b) Blow-out

Figure 9. Velocity development of blow-out along the center vertical axis of the tunnel face of case 2 (unit: m/step).

velocity evolution of the monitored points along the center vertical axis of the tunnel face, as shown in Figure 9.

5 COMPARISON OF FAILURE MECHANISMS

The failure mechanisms of five-block model and 3D numerical modeling are compared in case 2 (as shown in Figure 10). In five-block model, two sets of α and β_i are obtained by optimization of the coefficients N_γ and N_s. As shown in Figure 10, there are only small differences between the two soil mass at failure corresponding to the two sets of α and β_i.

Basically speaking, the failure mechanisms of five-block model and 3D numerical modeling well agree with each other. Both of them well predict the partial failure on the upper part of the tunnel face in blow-out, and global failure of whole tunnel face in collapse.

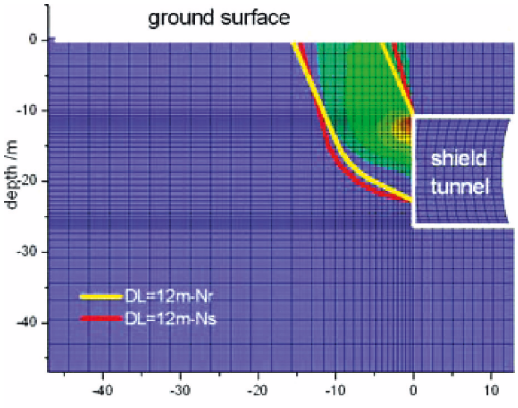

(a) Blow-out

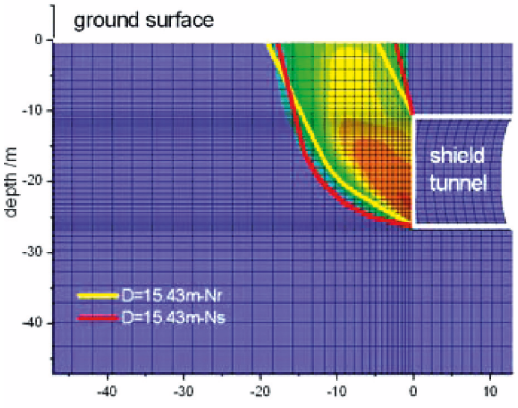

(b) Collapse

Figure 10. Comparison of failure mechanisms of Case 2 (velocity contour for FLAC^{3D} analysis).

Table 2. Comparison of critical slurry pressure at tunnel center level in case 2.

	Critical slurry pressure /kPa		Pressure factor M	
	Collapse	Blow-out	Collapse	Blow-out
5-Block Model	358.5	712.5	0.67	1.33
3D Numerical	376.3	698.9	0.70	1.30

6 CONCLUSIONS

1. Both the results of partial failure mechanism based on multiblock model and 3D numerical analysis show that the partial failure mechanism will happen in blow-out but global failure with entire tunnel face will dominate the collapse failure, especially in case where cohesion is changing with depth.
2. The critical slurry pressures of both multiblock partial failure mechanism and 3D numerical analysis are as shown in Table 2. The results well agree with each other. It should be noted that the multiblock model is the upper-bound solution; it is possible that a smaller value of the critical slurry pressure for blow-out and greater one for collapse could be found.

3. The results of 3D numerical analysis show that, in blow-out, the failure area on the tunnel face is described by an elliptic shape, with a long axis in horizontal direction, and a short axis in vertical direction. However, this shape of failure mechanism is different from the assumption of the multiblock model of upper-bound theorem, which is an elliptic shape with long axis in vertical direction.
4. In multiblock model analysis of case 2, a mean value of cohesion c_u from the top to the bottom of the failure block is employed. However, according to the shape of the failure block, the changing cohesion will influence the energy dissipation along the lateral surface of failure block. A more precise calculation of energy dissipation along the failure surface with c_u changing with depth is necessary to take into account. Also, the rotation of failure block caused by the eccentricity of the slurry pressure should be considered in multiblock model to obtain better results.

ACKNOWLEDGEMENTS

The research were conducted with funding provided by the National High Technology Research and Development Program (863 Program) of China and Shanghai Leading Academic Discipline Project, Project Number: B308. The first author is grateful to EGIDE to provide the French funding scholarship of her doctoral stay in INSA Lyon. Particular thanks are due to Prof. Soubra. A. H. for important discussion and the use of multiblock software.

REFERENCES

Anagnostou, G. & Kovári, K. 1994. The Face Stability of Slurry-Shield-Driven Tunnels. *Tunnelling and Underground Space Technology.* Vol.9, No. 2:165–174.

Broere, W. 2001. *Tunnel Face Stability & New CPT Applications.* PhD thesis, Delft University of Technology. Delft University Press, the Netherlands.

Chambon, P. & Corté, J.F. 1994. Shallow tunnels in cohesionless soil: Stability of tunnel face. *ASCE Journal of Geotechnical Engineering*. 120: 1148–1165.

Davis, E.H., Gunn, M.J., Mair, R.J. & Seneviratne, H.N. 1980. The Stability of Shallow Tunnels and Underground Openings in Cohesive Material. *Geotechnique.* 30 (4): 397–416.

Gioda, G. & Swoboda, G. 1999. Developments and Applications of the Numerical Analysis of Tunnels in Continuous Media. *International Journal for Numerical and Analytical Methods in Geomechanics*. 23: 1393–1405.

Horn, M. 1961. Horizontal earth pressure on perpendicular tunnel face. Hungarian National Conference of the Foundation Engineer Industry, Budapest. (In Hungarian)

Leca, E. & Dormieux, L. 1990. Upper and lower bound solutions for the face stability of shallow circular tunnels in frictional material. *Géotechnique* 40, 4: 581–606.

Soubra, A.H. 2000. Three-dimensional face stability analysis of shallow circular tunnels. *International Conference on Geotechnical and Geological Engineering, 19–24 November 2000*. Melbourne, Australia.

Soubra, A.H. 2002. Kinematical approach to the face stability analysis of shallow circular tunnels. *8th International Symposium on Plasticity*, 443–445. Canada, British Columbia.

Subrin, D. & Wong, H. 2002. Tunnel face stability in frictional material: a new 3D failure mechanism. *C. R. Mecanique,* 330: 513–519. (In French)